Interaction between HVAC - HVDC System: Impact of Line Length on Transient Stability

D T Oyedokun
Dept of Electrical Eng
University of Cape Town
davoyedokun@ieee.org

K A Folly
Dept of Electrical Eng
University of Cape Town
komla.folly@uct.ac.za

A V Ubisse
Dept of Electrical Eng
University of Cape Town
avubisse@hotmail.com

L C Azimoh
Dept of Electrical Eng
University of Cape Town
leonard.azimoh@.uct.ac.za

***Abstract*- Amid the increasing need to implement more HVDC transmission schemes within the next two decades in South Africa, which is aimed at strengthening the existing HVAC transmission network and to enable the transfer of increased bulk power across the country, this paper seeks to highlight some of the issues that the power industry may be faced in terms of power system stability. In this paper, the transient stability analysis of a power system made of four generating plants and hybrid HVAC-HVDC transmission line is investigated. The length of the HVAC line will be fixed at a pre-specified value (i.e., 500km), while the HVDC line length is varied from 100 km to 3,000 km. DC line faults and AC line 3-phase faults are applied to the system to determine its resilience to transient instabilities at the different HVDC line lengths. The simulation results show that the use of longer HVDC transmission line in parallel with a HVAC transmission line improves the stability of the system after a DC transmission line fault occurs in the system. However, the HVDC line length does not have a significant impact on the stability of the system after a 3-phase fault occurs on the HVAC transmission line.**

***Index Terms*—Rotor angle stability, transient stability, interconnection, HVAC- HVDC power system, AC and DC faults.**

I. INTRODUCTION

Modern power transmission systems are experiencing increased complexity in a bid to satisfy the growing power demand. Larger nuclear, coal and renewable energy plants are commissioned across the globe annually to increase the amount of power available for transmission and distribution. With countries like China, South Africa and Russia engaging in progressive steps to increase the generating and transmission capacity, and stability margins to meet increasing demand, there is a need to provide suitable and reliable transmission schemes that are cost effective with lower losses and higher stability margins [1]. Historically, HVAC was used for long distance power transmission. However, stability and transmission efficiency challenges led to the development and advancement of HVDC technology. To a great extent, HVDC transmission is able to overcome the challenges faced by HVAC in long distance transmission [2,3,4,5]. As a result, in many countries, HVDC transmission lines are adopted. The increasing use of HVDC transmission lines led to a new challenge in power systems, which is the interaction of HVAC and HVDC transmission systems with respect to power system stability. Stability which has been an underlying problem in the operation of power systems and can be dated back as far as 1912 [6], is defined as the ability of a power system, for a given initial operating condition, to regain a state of operating equilibrium subsequent to being subjected to a fault, with most system variables bounded so that practically the complete system remains intact [6]. These disturbances range from small disturbances such as small and continuous changes in the generator electrical output and loads to larger disturbances such as outage of transmission lines and generators; three phase AC and DC faults, etc.. It has been shown that the use of HVDC transmission lines in parallel with HVAC transmission lines increases the strength and the stability margins of the system. An example of such interconnection is the Pacific Intertie in California and Oregon [7, 8]. As faults cannot be completely avoided, it is imperative for power system engineers to determine the impact of AC and DC faults on the stability of the entire power system [9, 10]. In this paper, the impact of HVAC and HVDC line faults on the transient stability of the entire system is investigated with respect to the length of the HVDC transmission line.

II. ROTOR ANGLE STABILITY

A. Rotor Dynamics and Swing Equation

Rotor angle stability is the ability of synchronous machines in a power system to remain in synchronism after been subjected to a disturbance. It depends on the ability of the machines to maintain equilibrium between the electromagnetic torque and the mechanical torque. The movement of the rotor is governed by the Newton's second law of motion as given by equation 1 [3, 11].

$$\frac{2H}{\omega_0}\frac{d^2\delta}{dt^2} = P_m - P_e \qquad (1)$$

where
H is the per-unit inertia constant in sec
δ is the rotor angle in *rad*.

ω_0 is the synchronous speed in rad/sec.

P_e is the electrical torque in per unit
P_m is the mechanical power in per unit.

When the power system is in steady state of equilibrium, the mechanical power and the electrical power of the generator in (1) remain the same [6]. Hence, there is no accelerating power. This means that the rotor angle of the synchronous machines in the interconnected power system will be at a fixed angular position. If the systems is perturbed by a disturbance such as a three-phase AC fault, DC line fault or the loss of a generating unit, the equilibrium between P_e and P_m is lost and the speed of the generator changes. This change will lead to an imbalance in the active power generation by all the machines in the power system [3, 6, 11, 12, 13].

B. *System Responses to AC and DC Fault*

The stability of such power systems containing HVDC transmission schemes are affected by DC line faults, converter faults, etc. In AC systems, relays and circuit breakers are used for fault detection and clearance. On the contrary, most of the faults in DC systems are self-clearing or are cleared through the action of converter controls [3]. In some cases, it may become necessary to take out a bridge or an entire pole out of service. The most common type of faults on DC lines is pole-to-ground faults. This fault blocks power transfer on the affected pole with the rest poles remaining intact. During this fault, the short circuit causes the rectifier current to increase while the inverter current decrease. The rectifier current control acts to reduce the direct voltage and also reduce the current back to the current set point (normal operation current level). At the inverter side, the current level reduces below its current reference value. This causes the inverter to change from Constant Extinction Angle (CEA) control to Constant Current (CC) control. As a result, the voltage of the inverter reduces to zero and then reverses its polarity. Typically, the total time it takes for fault clearance and return to service is between 200 ms to 300 ms. The DC system response to AC fault is faster than that of the AC system. The DC system is capable of self sustenance through the AC system fault or in severe cases, there will be a reduction in power or a complete shutdown till the AC system recovers from the fault. When the AC fault is a distant 3-phase fault, there will be a reduction in the rectifier commutation voltage, which will lead to a reduction in the DC voltage and current. If the firing angle reaches its minimum value, the control measure will switch the rectifier from CC mode to Constant Ignition Angle (CIA) mode while the inverter changes to CC mode. Although in theory, DC power may be transmitted via the HVDC transmission line when the rectifier voltage is very low, the resulting increase in reactive power consumption could damage the generators. This is mainly because the inverter would have to change from CEA to CC mode by lowering its voltage and increasing β [14, 15, 17, 18].

III. System Model and Simulation Results

A. *Power System Model*

DigSILENT power factory was used in the simulations. Figure 1 shows the power system that was used in the simulations. There are four generators located in two areas; each has a capacity of 1800 MVA. In addition, area 2 has two distribution centres. The first distribution centre is at bus 7. This bus is connected to bus 5 via a 1600 MVA 500/11 kV step down transformer. The second distribution centre is at bus 8 which is connected to bus 5 via a 1,600 MVA 500/11 kV step down transformer. The load at bus 7 is 1,064 MW while the load at bus 8 is 1379 MW. Capacitor banks are connected to bus 5 and Bus 6 and contribute a total reactive power compensation of 1000 Mvar. In the following sub-sections, the impact of AC three-phase fault and DC line fault with respect to varying HVDC line length on the transient stability is investigated. First the DC fault is applied at the middle of the HVDC transmission line while the HVDC line length is varying. The same scenario is considered when there is a three-phase AC fault on the HVAC transmission line occurs in the system

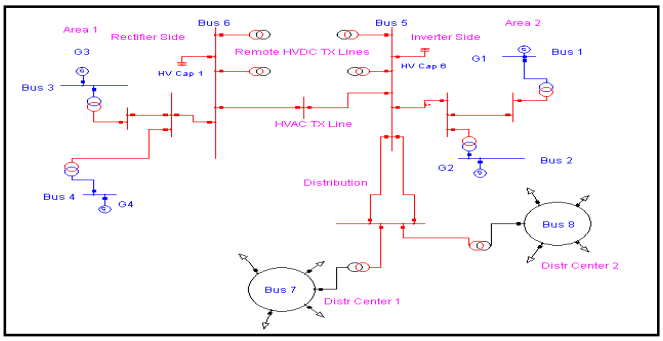

Fig. 1. Power Network used in the simulations

B. *DC Fault on HVDC Transmission line*

In this section, the effect of a HVDC transmission line fault on the transient stability of the system is investigated. A 50 ms DC fault is applied at 50 % of the HVDC transmission line. The length of the HVAC line is fixed at 500 km, while the length of the HVDC line is varied between 100 km and 3,000 km. Figure 2 shows the rotor angle of G2. It can be seen that the pre-fault rotor angle of G2 decreases (i.e. the absolute value decreases) as the length of the HVDC transmission line increases. Also, the amplitude of the rotor angle oscillations decreased with the increase in the HVDC transmission line length. After the fault was cleared, it took on average about 20 seconds for the rotor angle to stabilize when the HVDC transmission line length is less than 3000 km. When the HVDC line length is 3000 km, it took about 16 seconds for the rotor angle to settle down. This is expected because, as the length of the transmission line increases, the

distance between the fault and G2 increases. Therefore, the effect of the fault of G2 reduces.

Figure 3 shows the active power generated at G2. At steady state, G2 generated about 400 MW. At the time of the fault, the active power generation increased from 400 MW to about 1,300 MW to compensate for the reduction of power transmitted from area 1 due to the fault. After the fault was cleared, the active power oscillated between 500 MW and 300 MW before reaching its pre-fault value of 400 MW. The amplitude of the active power oscillations was the lowest when the HVDC line was at 3000 km. However, at this line length, the system experienced a dip in active power after the fault occurs. The time taken for the active power to reach its pre-fault value was the same for all the HVDC transmission line lengths.

Figure 4 shows the terminal voltage at G2. It can be seen that before the fault, the terminal voltage was 1.0 p.u. During the fault, the terminal voltage increased to 1.03 p.u. before it dipped to 0.98 p.u. Then the voltage oscillated between 1.03 p.u. and 0.98 p.u. before settling to 1.0 p.u. after the fault was cleared. The largest dip in terminal voltage was experienced at 100 km, while the largest post fault oscillations occur at 1,500 km line length. At 3000 km, the system experiences the smallest terminal voltage oscillations. The time taken for the terminal voltage to settle was about 18 seconds, which is found to be the same across all transmission lines.

Figure 5 shows the reactive power generated at G2. From fig. 5, it can be seen that the amount of reactive power generated by G2 decreases as the length of the HVDC transmission line increases. Similarly, the amplitude of the reactive power oscillation and the time taken to reach steady state also reduced as the length of the HVDC transmission line increased. For the 3,000 km HVDC transmission line, the reactive power generation settled to steady state at 15 seconds as compared to about 18 seconds for HVDC line length smaller than 3000 km.

Figure 6 shows the rotor angle oscillation at G3. It can be seen that the rotor angle decreased from -37^0 to -43^0 with the increase in the length of the HVDC transmission line. Also, the amplitude of the rotor angle oscillations and the time taken to reach steady state decreased with the increase in length of the HVDC transmission line. This is similar to the rotor angle of G2 as depicted in fig. 2. However, the amplitude of the rotor angle oscillations at 1500 km was found to be greater than the rotor angle oscillation at 500 km.

Figure 7 shows the active power generation at G3. At steady state, G3 generated 1,000 MW. At the time of the fault, the active power generation increased from 1000 MW to about 2,200 MW. After the fault was cleared, the active power dropped to 440 MW before oscillating between 1,100 MW and 900 MW. At about 12 seconds, the active power stabilized at 1,000 MW. The active power had the lowest dip when the HVDC line was 3,000 km. The time taken for the active power to reach its pre-fault value was the same for all the HVDC transmission line lengths.

Figure 8 shows the terminal voltage at G3. The effect of the DC fault on the terminal voltage at G3 reduced as length of the transmission line increased as seen in figure 8. At 3,000 km, the voltage dipped by 0.8 pu while it dipped to 0.41 pu at 100 km. This clearly shows that the long line length has a positive effect on voltage level during the fault.

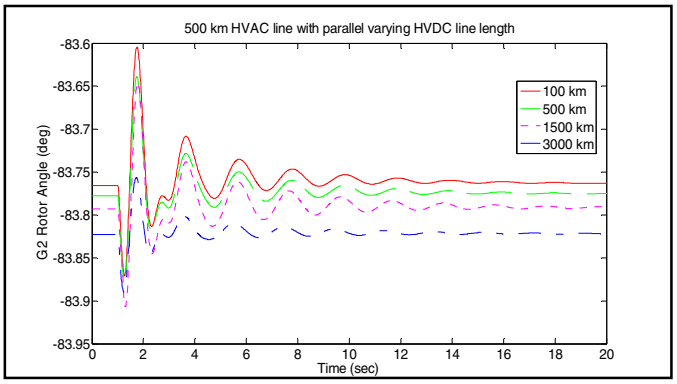

Fig. 2. HVDC Line Fault: Rotor Angle of G2

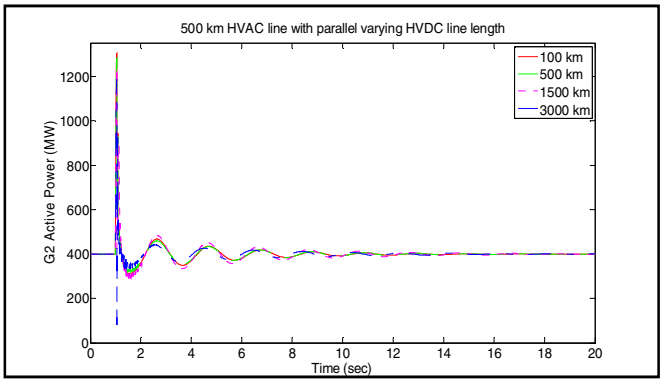

Fig. 3. HVDC Line Fault: Active Power generated by G2

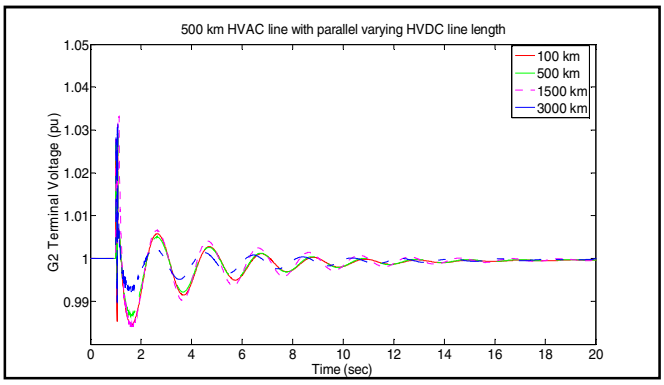

Fig. 4. HVDC Line Fault: G2 Terminal Voltage

For all the four HVDC transmission line lengths, the terminal voltage settled in 7.5 seconds.

Figure 9 shows the reactive power at G3. From this figure it can be seen that the amount of reactive power generated by G3 decreases at the length of the HVDC transmission line increases. Similarly, the amplitude of the reactive power

oscillations and the time taken to reach steady state reduced as the length of the HVDC transmission line increased. After the fault is cleared, it took about 8 seconds for the reactive power to reach steady state with the 3,000 km HVDC transmission line, while it took about 10 seconds with the 100 km HVDC transmission line.

C. Three-Phase fault on HVAC Transmission Line

In this section, a three phase fault was initiated at 50 % of the HVAC transmission line for 50 ms. The HVAC transmission line is fixed at 500 km, while the length of the HVDC line is varied between 100 km and 3,000 km as before.

Figure 10 shows the rotor angle of G2. The rotor angle decreased from -83.77^0 to -83.83^0 with the increase in the length of the HVDC transmission line. During the fault, the rotor angle of G2 oscillated between -83.61^0 and -83.85^0 across the four transmission lines before reaching steady state. The amplitude of the rotor angle oscillations and the time taken to reach steady state increased with the increase in length of the HVDC transmission line.

Figure 11 shows the terminal voltage of G2. The results of the terminal voltage in fig. 11 show that the HVDC transmission line length has no impact on the terminal voltage dip at G2 during the 3-phase to ground fault on the HVAC transmission line.

Figure 12 shows the active power generation at G2. It can be seen that before the HVAC line fault, G2 was generating 400 MW. The highest increase in active power generation during the fault is with the 100 km HVDC transmission line. Although the time taken for the active power to stabilize using the four HVDC transmission line was the same, the amplitude of the active power oscillation increased with the increase in the length of the HVDC transmission line.

Figure 13 shows the reactive power generated at G2. The reactive power generation reduced with the increase in the HVDC transmission line length. Furthermore, the time taken for the reactive power to stabilize increased with the increase in the HVDC transmission line length. It took 6 seconds faster to stabilize when the HVDC transmission line was 100 km as compared to 3,000 km.

Figure 14 shows the rotor angle of G3. The pre-fault rotor angle reduced from -36^0 to -37.5^0 as the length of the HVDC transmission line increased from 100 km to 3,000 km. During and after the fault, the amplitude of the rotor angle oscillations of G3 increased with the increase in the HVDC transmission line.

Figure 15 shows the terminal voltage at G3. The terminal voltage oscillations at G3 did not vary with the change in the HVDC transmission line length when the 3-phase fault occurred on the HVAC transmission line.

Figure 16 shows the active power of G3. Before the fault, the active power generation was 1,000 MW. During the fault, the active power generation reduced to 460 MW as expected.

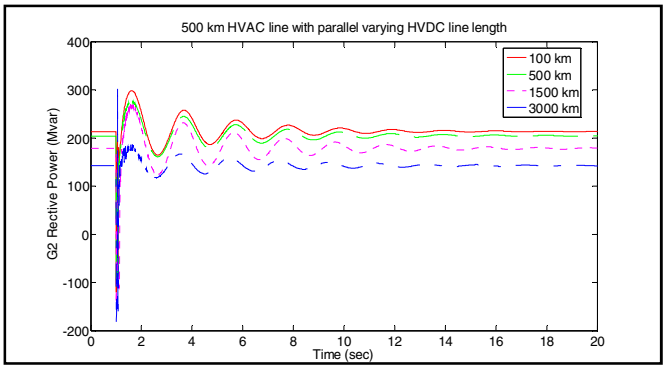

Fig. 5. HVDC Line Fault: Reactive Power generated by G2

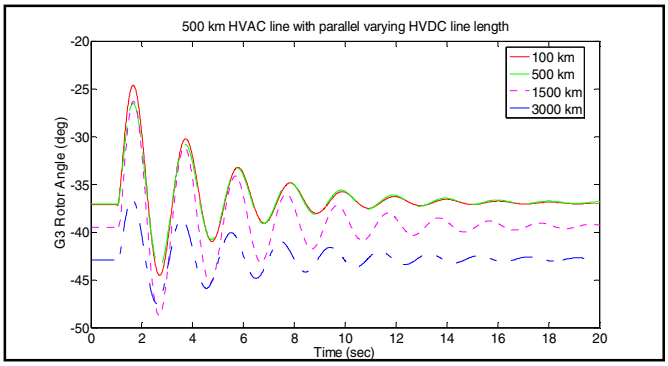

Fig. 6. HVDC Line Fault: Rotor Angle of G3

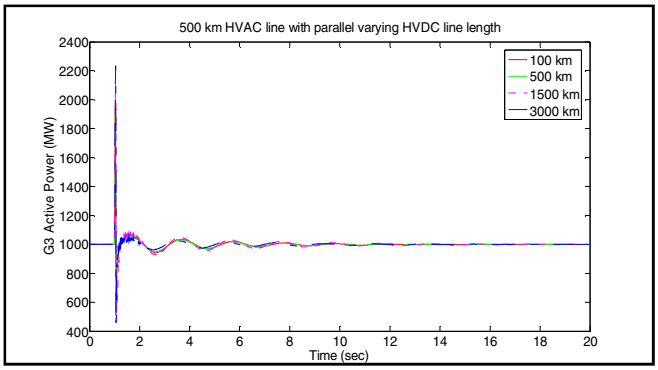

Fig. 7. HVDC Line Fault: Active Power generated by G3

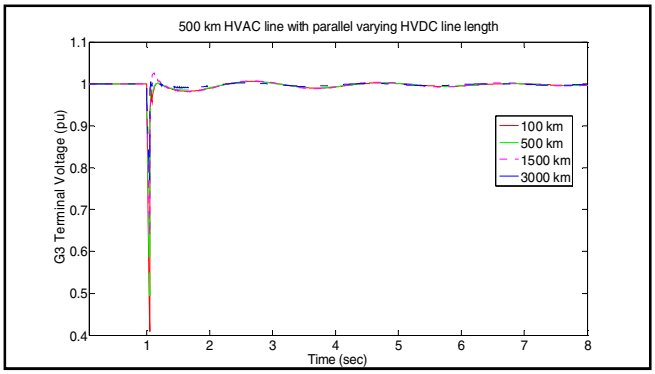

Fig. 8. HVDC Line Fault: Terminal Voltage at G3

This is because the amount of power transmitted via the HVDC line is fixed. G2 generated 230 MW while G1 generated 310 MW to compensate for the 540 MW lost from G3 during the fault on the HVAC transmission line. The active power oscillations at G3 are fairly independent of the length of the HVDC transmission line as seen in figure 16. The time taken for the active power to reach its pre-fault value was the same for all the HVDC transmission lines.

Figure 17 shows the reactive power generation at G3. The pre-fault reactive power generation at G3 decreased with the increase in the HVDC transmission line length. During the fault, the reactive power generation increased from 190 Mvar to 1,200 Mvar (for the 100 km HVDC transmission line). However, the time taken for the reactive power to stabilize increased with the increase in the HVDC transmission line length. There was no significant impact of the HVDC transmission line length on the amplitude of the reactive power oscillations at G3.

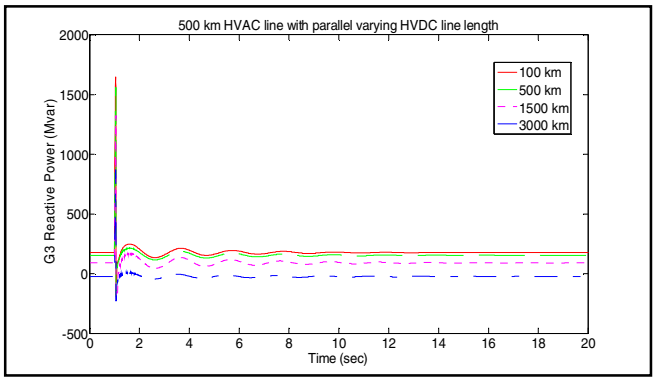

Fig. 9. HVDC Line Fault: Reactive Power generated by G3

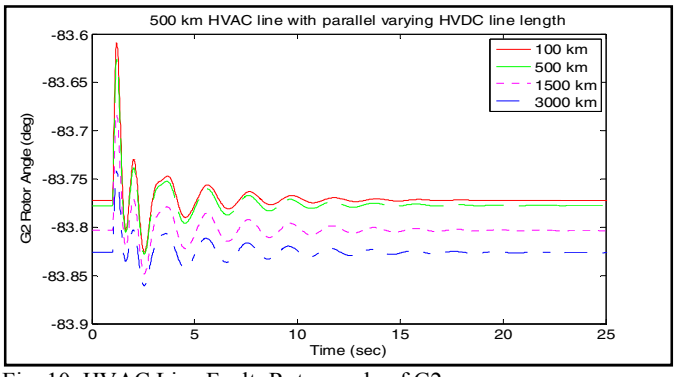

Fig. 10. HVAC Line Fault: Rotor angle of G2

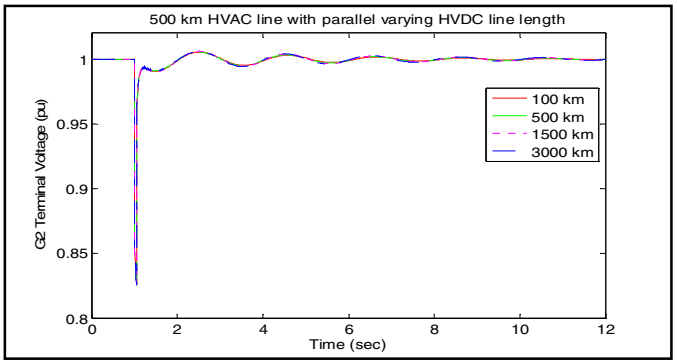

Fig. 11. HVAC Line Fault Terminal Voltage at G2

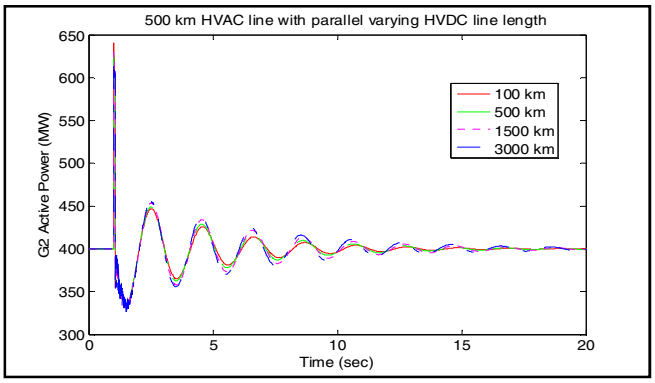

Fig. 12. HVAC Line Fault Active Power generated at G2

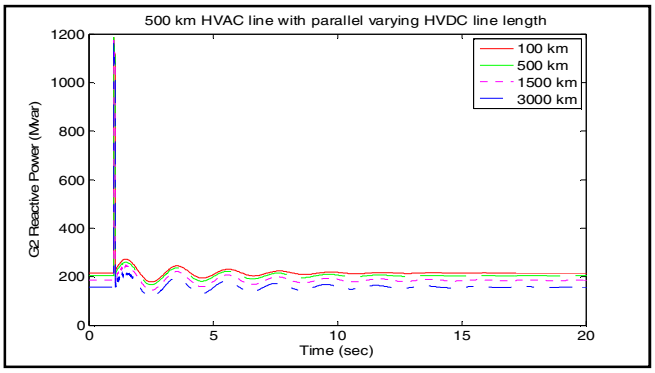

Fig. 13. HVAC Line Fault Reactive power generated at G2

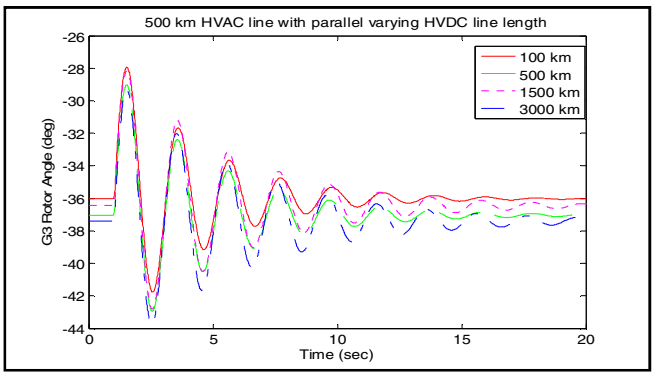

Fig. 14. HVAC Line Fault Rotor angle of G3

IV. CONCLUSIONS

The simulation results suggest that the transient stability of the system after a DC transmission line fault is improved when longer HVDC transmission lines are used in parallel with a relatively shorter HVAC transmission lines. It was also observed that the generator terminal voltage dip is reduced with the increasing length of the HVDC transmission line. However, for a three-phase fault the above observation does not hold. The terminal voltage dip is not dependent on the length of the HVDC transmission line. Also, the additional reactive power generated by G2 was higher after the 3-phase fault on the HVAC transmission line when compared to the reactive power generated by G2 after the DC line fault. More studies need to be done in the future to fully understand the different behaviour of the system under both AC and DC faults.

REFERENCES

[1]. SIEMENS, " International Workshop for 800 kV High Voltage Direct Current (HVDC) Systems", New Delhi- India, 25th -26th Feb, 2005.

[2]. D. T. Oyedokun, K.A Folly, "Power Flow studies in HVAC and HVDC Transmision Lines" , IASTED AfricaPES 2008, Garborone, Botswana, 2008.

[3]. P Kundar, *Power System Stability and Control,* McGraw-Hill, Inc: Newyork: 1993.

[4]. M Hausler, "Multi terminal HVDC for High Power transmission in Europe", CWPEX99, Pozan, Poland, March 1999.

[5]. G. M. Huang, V. Krishnaswamy, "HVDC Controls for Power System Stability", Power Engineering Society Summer Meeting, Vol. 1. 25th July, 2002.

[6]. P. Kundur, J. Paserba, V. Ajjiarapu, G. Andersson, A. Bose, C. Canizares, N. Hatziargyriou, D. Hill, A. Stankovic, C.Taylor, Van T. Cutsem, and V. Vittal, "Definition and classification of power system stability - IEEE/CIGRE Joint Task Force on Stability Terms and Definitions, " IEEE Trans. on Power Systems, Vol.19, No. 2, pp. 1381 -1397, May, 2004.

[7]. F. F Wu, "Technical Considerations for Power Grid Interconnection in Northeast Asia", University of Hong Kong and California at Berkely, http://www.nautilus.org/archives/energy/grid/abstracts/wu_technical.pdf , April 27th, 2009.

[8]. D.T. Oyedokun, K. A. Folly, S. P Chowdhury, "Effect of Converter DC fault on the Transient Stability of a Multi-Machine Power System with HVDC Transmission lines", IEEE Africon, Nairobi, Kenya September 23rd -25th 2009

[9]. S. Arabi, P. Kundur, J. H. Sawada, "Approximate HVDC Transmission Simulation Models for Various Power System Stability Studies", IEEE Transaction on Power Systems, Vol. 13, No. 4. November, 1998.

[10]. H. Zhaoquing, M. Chengxiong, L. Jiming, "Improvement of Transient Stability in AC System by HVDC Light", IEEE/PES Transmission and Distribution Conference & Exibition: Asia and Pacific. Dalian, China, 2005

[11]. D. A. Woodford , *HVDC transmission,*. Canada: Manitoba HVDC Research Center, pp. 1-25, 1998.

[12]. M. P. Bahrman, "The ABCs of HVDC transmission technologies", IEEE Power and Energy Magazine, pp. 33-44, March/April 2007.

[13]. K. Ijumba, "Effect of AC line Length on the Stability of the AC/DC interconnection". Bsc (Elec Eng) Thesis, University of Cape Town, 2005.

[14]. D. Gao, *AC Transmission Lines and Underground Cables*, Tennessee Tech University, 2008.

[15]. EPRI Report EL-3004, "Methodology for Integration of HVDC Links in Large AC Systems- Phase 1: Reference Manua", New York: Ebasco Services, 1983.

[16]. J. Arrillaga, *High Voltage Direct Current Transmission*, London: Peter Peregrinus 1983, pp. 149-151.

[17]. K.R. Padiyar, *Analysis of Subsynchronous Resonance in Power Systems*, Boston: Kluwer Academic Publishers 1999, pp. 181.

[18]. P.K. Dash, A. Routry, and A. C. Liew, "Design of an energy function based fuzzy tuning controller for HVDC Links," Electrical Power and Energy Systems, pp. 337 -347, No. 21, 1999.

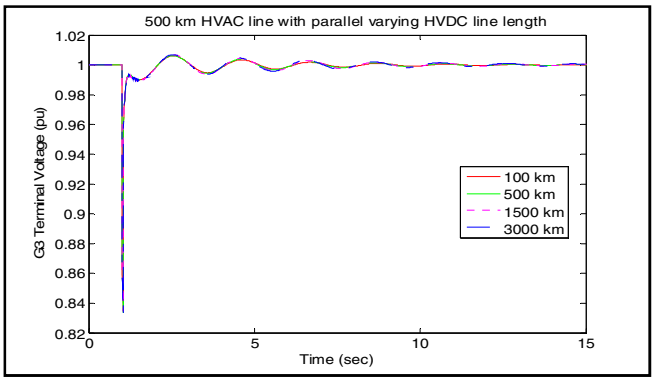

Fig. 15. HVAC Line Fault Terminal Voltage at G3

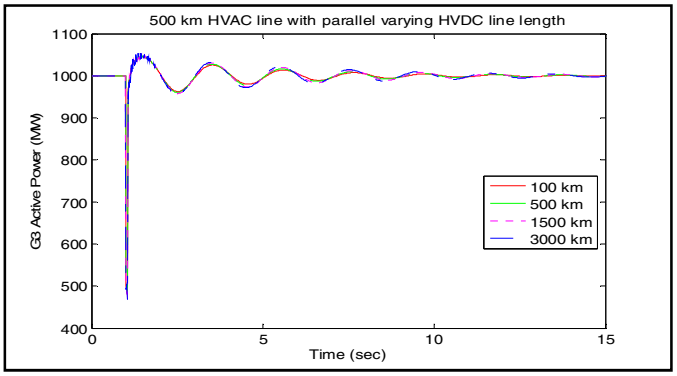

Fig. 16. HVAC Line Fault Active Power generated at G3

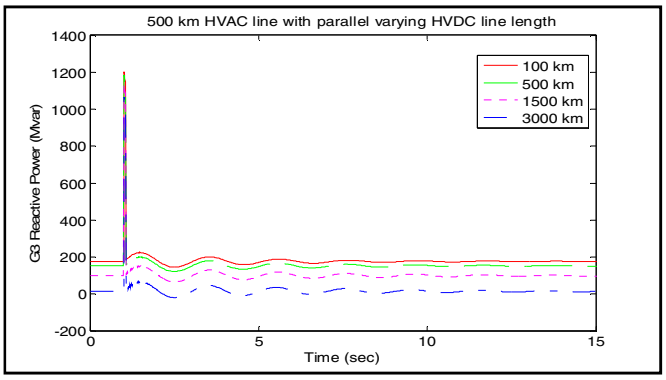

Fig. 17 HVAC Line Fault Reactive Power generated at G3